Comment on "A study of the slope probability density function of the ocean waves from radar observations" by D. Hauser et al.

Paul A. Hwang[1]

Received 1 July 2008; revised 23 October 2008; accepted 2 December 2008; published 12 February 2009.

Citation: Hwang, P. A. (2009), Comment on ''A study of the slope probability density function of the ocean waves from radar observations'' by D. Hauser et al., *J. Geophys. Res.*, *114*, C02008, doi:10.1029/2008JC005005.

1. Introduction

[1] Intermediate-scale waves (ISW, about 0.02 to 6 m long) are the main contributor of the ocean surface roughness relevant to passive and active microwave remote sensing of the ocean. While wind speed is the most important parameter determining the spectral composition of the ocean surface roughness, analysis of field measurements indicates that the wave spectrum of ISW is strongly modified by background waves. The mean square slope derived from the wave spectrum is, therefore, also modified by the background wave condition. Investigation of ocean surface roughness without taking into account the sea state parameter can lead to incorrect conclusions.

[2] The paper by *Hauser et al.* [2008] (hereinafter referred to as *HCGM08*) presented very interesting results on the properties of ocean surface roughness derived from C-band (5.35 GHz) radar observations. They compared the filtered mean square slope obtained under the assumption of Gaussian probability density function (pdf) of surface slopes with three published spectral models. Their interpretation of the empirical spectral model of *Hwang* [2005] (hereinafter referred to as *H05*) is inaccurate. As a result, they attributed the disagreement between their data with *H05* to the discontinuity in the *H05* spectrum caused by matching the empirically parameterized intermediate-scale wave (ISW) spectrum and an assumed equilibrium spectrum for the longer waves. The issue of matching will be further discussed in Section 2. Their description on the comparison with *H05* was verbal (*HCGM08*, p. 9), the result is shown in Figure 1 here. The analyses of *HCGM08* produced two sets of mean square slope (mss) as a function of wind speed based on the assumption of Gaussian (shown in their Figure 6d) and non-Gaussian (their Figure 11b) surface slope pdf. They have noticed the large difference between the two sets of mss but no further comment or explanation was offered. Derivation of ocean surface roughness from radar backscattering cross section is a complex topic. Extensive discussions on the subject have been given in earlier publications [e.g., *Jackson et al.*, 1992; *Walsh et al.*, 1998]. Results of mss computation using essentially the same approach of *HCGM08* by *Jackson et al.* [1992] for Ku band (14 GHz) and *Walsh et al.* [1998] for Ka band (36 GHz) are also shown in Figure 1, together with the sun glitter data of *Cox and Munk* [1954] and the filtered mss of *H05* spectral model integrated to an upper cutoff wave number, k_c, suggested by *Jackson et al.* [1992]. This cutoff wave number corresponds to surface wavelength about 4.7 times the radar wavelength. The cutoff wave number used by *HCGM08* is much higher (corresponding to surface wavelength about 2.2 times the radar wavelength). For their C-band radar frequency (5.35 GHz), k_c is 24 rad/m on the basis of the criterion of *Jackson et al.* [1992] and 51 rad/m on the basis of *HCGM08*. Also shown in their Figure 1 are the filtered mean square slope derived from direct inversion of the backscattering cross section of Ka band radar reported by *Vandemark et al.* [2004]. Further discussion of these data is deferred to Section 3.

[3] After a close examination of their experimental conditions, it becomes clear that the source of disagreement is quite different from that suggested by *Hauser et al.* and the hint was in fact given in *H05*, that is, the mean square slope of the ocean surface is significantly modified by background waves. *HCGM08* did not provide too much information about the wind and wave conditions of their experiment. However, on the basis of the tabulated data presented in an earlier paper of the same experiment [*Mouche et al.*, 2005], the wavefields are strongly influenced by swell not related to the local wind condition. In contrast, the database used in constructing the *H05* spectrum is wind-sea dominant with mild swell presence (Section 3). Because radar remote sensing plays an increasingly more important role in oceanographic research and environmental monitoring, and that an accurate interpretation of the remote sensing measurement requires a correct understanding of the ocean surface roughness in response to various geophysical parameters of interest, such as wind, air-sea stability condition, waves of various scales and currents of various sources, a clarification of the properties of the ocean surface roughness spectrum is important. I hope this note serves to correct the misinterpretation given by *Hauser et al.* [2008] regarding the ocean surface roughness spectrum and to call attention the important role of a missing parameter – the background wave condition – in their analysis.

2. Surface Roughness Spectrum

[4] In an analysis of the source function balance of short ocean surface waves, *Phillips* [1984] presented a compelling argument on the importance of establishing the functional

[1]Remote Sensing Division, Naval Research Laboratory, Washington, DC, USA.

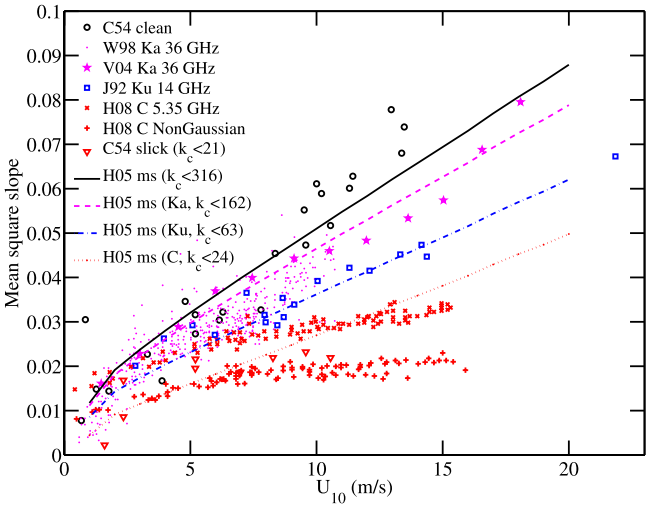

Figure 1. Filtered mean square slopes as a function of wind speed based on measurements of airborne radars with different frequencies. [*Jackson et al.*, 1992; *Walsh et al.*, 1998; *Vandemark et al.*, 2004; *Hauser et al.*, 2008] and sun glitter analysis [*Cox and Munk*, 1954]. The smooth curves are the corresponding mss obtained from integration of the wave number spectral model (mixed sea condition) of *Hwang* [2005] with the upper cutoff wave number defined by *Jackson et al.* [1992]. J92, *Jackson et al.* [1992]; W98, *Walsh et al.* [1998]; V04, *Vandemark et al.* [2004]; H08, *Hauser et al.* [2008]; C05, *Cox and Munk* [1954]; H05, *Hwang* [2005].

relationship between the dimensionless wave spectrum $B(k)$ and dimensionless wind speed u_*/c, where k is wave number, u_* wind friction velocity and c wave phase speed: the source terms of wind input and wave dissipation are ultimately expressed as functions of B and u_*/c, so a quantitative knowledge of $B(u_*/c)$ can provide a significant boost toward a better understanding of the source functions. Using fast response capacitance wave gauges mounted on a free drifting structure to minimize complication of Doppler frequency shift in deriving the wave number spectrum from time series of surface displacement, *Hwang and Wang* [2004] found that for each wave number component, $B(u_*/c)$ can be expressed as a power law function, that is, $B(u_*/c;k) = A_0(u_*/c)^{a_0}$, where A_0 and a_0 are functions of k. Using the data they collected from the ocean, the empirical dependence of $A_0(k)$ and $a_0(k)$ were obtained (Figures 2a and 2b) for the wavelength range between 0.02 and 6 m ($316 > k > 1$ rad/m). Their analysis indicates that background wave condition can modify $A_0(k)$ and $a_0(k)$ substantially, the results for the wind-sea and mixed sea subsets are shown with different symbols in Figures 2a and 2b. (They divided their collection of wave spectra into two subsets depending on the swell influence, which is quantified by a swell index defined by the ratio, R, of the spectral densities in the frequency bands $\omega < 0.6\ \max(\omega_p, \omega_0)$ and $\omega \geq 0.6\ \max(\omega_p, \omega_0)$, where ω is wave frequency, $\omega_0 = g/1.2U_{10}$ the expected minimum frequency of wind generated waves, ω_p the measured spectral peak frequency and g the gravitational acceleration. The first subset is dominantly wind waves with $R < 0.2$ and the second subset is swell influenced with $R \geq 0.4$.)

[5] Because c and k are related by the wave dispersion relation, $B(u_*/c;\ k)$ can be written as $B(k;\ u_*)$, which becomes a convenient parameterization function of the wave spectrum for the ISW that are important contributors of the ocean surface roughness [*Hwang*, 2005]. The empirical analysis of $B(u_*/c;\ k)$ by *Hwang and Wang* [2004] only covers the range $316 > k > 1$ rad/m. A simple equilibrium spectral wave model [*Phillips*, 1985] is added for the longer-scale waves. With this simple extension, conspicuous discontinuities are present at the matching wave number $k = 1$ rad/m. *Hwang* [2005] stated that the contribution of the mean square slope is dominated by the ISW and a relatively simple smoothing scheme such as linear interpolation using the spectral values at the two sides of the matching wave number can be adopted without causing significant impact on the integrated mean square slope.

[6] Alternatively, using the property that A_0 and a_0 approach their equivalent values of the equilibrium spectrum toward the long waves (0.052 and 1, respectively [e.g., *Phillips*, 1985; *Hwang et al.*, 2000]) as discussed in *H05*, the following asymptotic equations can be used for spectral computation in the range $k < 1$ rad/m,

$$A_0 = \begin{cases} 0.052e^{-0.6k}, & \text{wind sea} \\ 0.052e^{-0.7k}, & \text{mixed sea} \end{cases}, \tag{1}$$

and

$$a_0 = \begin{cases} e^{-0.2k}, & \text{wind sea} \\ e^{-0.15k}, & \text{mixed sea} \end{cases}. \tag{2}$$

[7] More elaborated extension functions toward both lower and higher wave number regions outside the range of field data are given by *Hwang* [2008]. As illustrated in Figures 2a and 2b, the asymptotic functions (1) and (2) provide a smooth match with the empirical data and the discontinuities of the resulting spectra are essentially eliminated (Figure 2c). The integrated mean square slopes for $k_c = 21$, 63, and 316 rad/m at wind speeds 5, 10, 15 and 20 m/s are shown in Figure 2d. These results are almost identical to those shown in Figure 3 of *H05* with the simple smoothing scheme. As expected, the method used to smooth the discontinuity in the neighborhood of the matching wave number does not introduce discernable difference in the filtered mss computation of microwave radar frequencies, in contradiction to the suggestion given by *Hauser et al.* [2008].

[8] A very noticeable feature of the wave number spectrum and filtered mean square slope shown in Figures 2c and 2d is the influence of background waves. This is the key point of this note and is further discussed in the next section.

3. Effect of Background Waves and Sea States of Various Data Sets

[9] In the absence of wave spectral information, a convenient way to characterize a wavefield is to examine the relationship between the dimensionless wave variance, $\eta_* = \eta_{rms}^2 g^2/U_{10}^4$, and dimensionless characteristic frequency, $\omega_* = \omega_p U_{10}/g$, where η_{rms} is the root mean square surface displacement. As

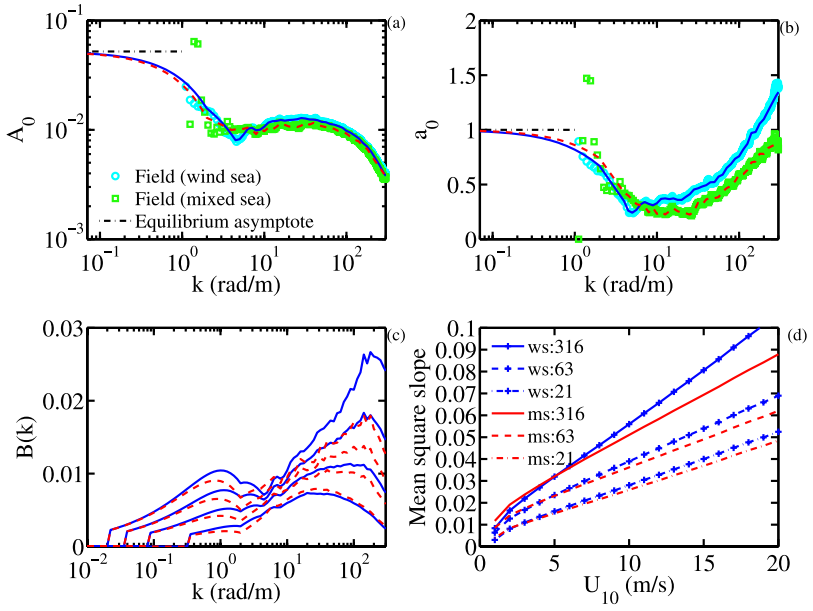

Figure 2. The (a) coefficient A_0 and (b) exponent a_0 of the dimensionless spectral parameterization function $B(k) = A_0(u_*/c)^{a_0}$ from analysis of field data [*Hwang and Wang*, 2004]; results based on wind sea and mixed sea are shown with light-colored symbols. The continuous curves are from look-up table [*Hwang*, 2005] and asymptotic equations (1) and (2) for low wave number extension. (c) Calculated wave number spectra at 5, 10, 15, and 20 m/s for wind sea (solid curves, wind speed increasing upward) and mixed sea (dashed curves). (d) The filtered mean square slope calculated with the spectra shown in Figure 2c for k_c = 21, 63, and 316 rad/m. Here ws indicates wind sea, and ms indicates mixed sea.

shown in Figure 3a (light-colored symbols), wave conditions in the field data used for the parameterization of the *H05* spectral model are predominantly underdeveloped wind generated waves with mild swell presence. The solid curve in Figure 3a represents the condition of duration- or fetch-limited wind generated waves [*Hwang*, 2006]. The horizontal dashed curve is $\eta_* = 3.6 \times 10^{-3}$ and the vertical dashed curve $\omega_* = 0.8$; the former is the empirically determined upper

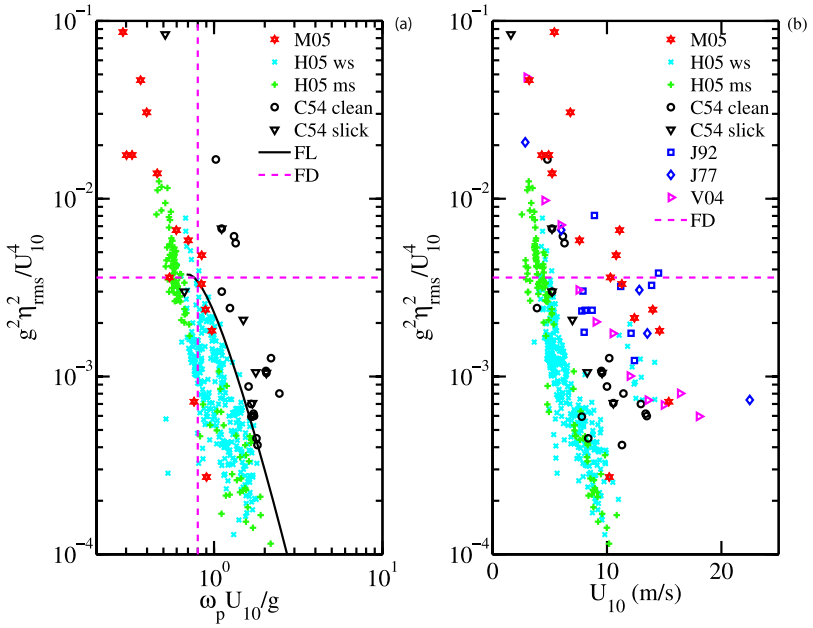

Figure 3. Sea state conditions of the data sets displayed in Figure 1 represented in terms of (a) dimensionless wave variance as a function of dimensionless peak wave frequency and (b) dimensionless wave variance as a function of reference wind speed. FL, fetch-limited; FD, fully developed; M05, *Mouche et al.* [2005]; J77, *Jones et al.* [1977]. Other shorthand notations are the same as those in Figure 1.

bound of the dimensionless wave variance, and the later the lower bound of the dimensionless wave frequency, of a fully developed wind-generated wavefield [e.g., *Young*, 1999; *Hwang*, 2006].

[10] Note that the swell index defined by *Hwang and Wang* [2004] is computed from the ratio of the spectral densities in the low- and high-frequency ranges (see Section 2). It does not have an equivalent representation using the bulk parameterization. This situation poses a serious challenge of trying to characterize the background wave conditions without the full knowledge of the surface wave spectrum, but as shown in Figure 3a most data points with $\eta_* > 3.6 \times 10^{-3}$ and $\omega_* < 0.8$ are also identified as mixed seas on the basis of the swell index derived from the spectral analysis. It is reasonable to expect that identifying wavefields with $\eta_* > 3.6 \times 10^{-3}$ or $\omega_* < 0.8$ as swell dominant should remain reliable.

[11] *HCGM08* only briefly discussed the wind and wave conditions in their experiment. More detailed information of the same experiment, including wind speed, wind direction, significant wave height, peak wavelength and air-sea temperature difference for 16 flights, each 2 to 3 hours long, were tabulated in an earlier paper [*Mouche et al.*, 2005]. Assuming that these tabulated data represent the conditions of *HCGM08*, it is found that the wave conditions deviate significantly from locally generated wind waves: the majority of the data are in the region of $\eta_* > 3.6 \times 10^{-3}$ or $\omega_* < 0.8$ (Figure 3a, hexagram symbol) and indicate strong swell presence. One of the key conclusions of *H05* is that with mild swell presence, the mss increases in low wind speed and decreases in high wind. If this trend persists, as we should expect from wave dynamic considerations [e.g., *Phillips and Banner*, 1974], then the strong swell condition of *HCGM08* is the true cause that their observed mss differ from those of *H05* in the fashion shown in Figure 1. It would be fruitful for *Hauser et al.* to look into the swell effects in their measurements. In this regard, it should be pointed out that the mss analysis of *HCGM08* yields a significant level of ambient mss (0.015) at zero wind speed. For reference, the mss magnitude at 15 m/s is about 0.03 in their data set. The ambient mss level is equivalent to a range of about ±10° fluctuation in the local incident angle of radar response to the locally wind generated roughness. (The existence of an equilibrium spectrum does produce a mss offset independent of wind speed [*Hwang and Wang*, 2001], also skewness of waveform produces a nonzero mss offset, but the magnitude is much smaller–about 0.005 and on the order of measurement uncertainty [*Cox and Munk*, 1954; *Bréon and Henriot*, 2006; *Munk*, 2009]). On the basis of their description of the experiment, the size of the radar resolution cell is approximately a ribbon of about 1.5 m in range and 280 to 420 m in azimuth. In the presence of strong swell, the effective incident angle of the resolution cell would be a complex function of the relative orientation of the radar look direction with respect to the swell propagation and the directional beam width of the swell system. How does this large change in local incident angle affect their retrieval of locally wind-generated roughness is less than straightforward to assess. (*Walsh et al.* [1998] present a comprehensive discussion on the tilting effect on the mss retrieval using their radar system with a relatively small circular or elliptical resolution cell. For a narrow ribbon resolution cell, the tilting effect is undoubtedly more complicated.) In their reanalysis of the *HCGM08* data given in the Reply with wind-sea and swell conditions sorted out, the ambient mss of the wind-sea subset (when extrapolated to zero wind speed) is even larger than that of the swell subset and the sensitivity to wind speed is stronger in the swell subset than in the wind-sea subset, both results defy a logic explanation and may reflect the difficulty in isolating the tilting effect for retrieving locally wind-generated surface roughness in the presence of long surface waves. To make the discussion of mss dependence on wind speed meaningful, the nonlocal contributions need to be removed from the processed result. The difficulty of obtaining uncontaminated mss in the low wave number region for investigating the wind speed dependence of wind-induced roughness is also seen in the laser altimeter data presented by *Vandemark et al.* [2004]. More detailed discussion on this issue is given by *Hwang* [2008].

[12] For reference, I also examined the sea state conditions of the other data sets shown in Figure 1. *Cox and Munk* [1954] tabulated detailed wind and wave information. The wave conditions in their experiment are wind-sea dominant with mild swell presence (Figure 3a). *Jackson et al.* [1992] listed only wind speed and wave height so η_* can be calculated but not ω_*. They also incorporated measurements of *Jones et al.* [1977, wind speed and wave height tabulated] and *Wentz* [1977, peak wave frequency or wave height not available], the data are mostly in the region with $\eta_* < 3.6 \times 10^{-3}$ (Figure 3b). *Vandemark et al.* [2004] also reported wind speed and wave height in graphic format (their Figure 4), the computed η_* is also mostly less than 3.6×10^{-3}. *Walsh et al.* [1998] only gave a plot of wind speed and wind direction along the flight track and no dimensionless wave parameter can be computed. Their experiment was conducted in the tropical ocean during the TOGA COARE experiment. The wave conditions are expected to be dominated by swell.

4. Concluding Remarks

[13] Intermediate-scale waves are the main contributor of the ocean surface roughness relevant to microwave frequencies. These waves are generated primarily by local wind but even mild swell can modify the spectrum of ISW considerably (Figure 2 and *Hwang* [2005]). The mean square slope calculated from integrating the wave spectrum is, therefore, influenced by the background wave condition. The wavefields in the paper by *Hauser et al.* [2008] deviate significantly from locally generated wind waves. The difference between the mean square slopes derived from their radar observations and from integration of *Hwang* [2005] spectrum is likely due to the strong swell influence in their experiment rather than the discontinuity in the simple spectral matching adopted by *Hwang* [2005], as they have suggested. In the presence of strong swell, the radar response to locally wind-generated roughness may be masked by the swell modification of the local incident angle because the radar resolution cell is tilted by the background swell. Retrieval of wind-generated roughness under such condition may present a considerable challenge.

[14] **Acknowledgments.** This work is sponsored by the Office of Naval Research (NRL work units 8027 and 8953 and program element 61153N; NRL contribution number NRL/JA/7260—08–0200).

References

Bréon, F. M., and N. Henriot (2006), Spaceborne observations of ocean glint reflectance and modeling of wave slope distributions, *J. Geophys. Res.*, *111*, C06005, doi:10.1029/2005JC003343.

Cox, C. S., and W. Munk (1954), Statistics of the sea surface derived from sun glitter, *J. Mar. Res.*, *13*, 198–227.

Hauser, D., G. Caudal, S. Guimbard, and A. A. Mouche (2008), A study of the slope probability density function of the ocean waves from radar observations, *J. Geophys. Res.*, *113*, C02006, doi:10.1029/2007JC004264.

Hwang, P. A. (2005), Wave number spectrum and mean-square slope of intermediate-scale ocean surface waves, *J. Geophys. Res.*, *110*, C10029, doi:10.1029/2005JC003002.

Hwang, P. A. (2006), Duration- and fetch-limited growth functions of wind-generated waves parameterized with three different scaling wind velocities, *J. Geophys. Res.*, *111*, C02005, doi:10.1029/2005JC003180.

Hwang, P. A. (2008), Observations of swell influence on ocean surface roughness, *J. Geophys. Res.*, *113*, C12024, doi:10.1029/2008JC005075.

Hwang, P. A., and D. W. Wang (2001), Directional distributions and mean square slopes in the equilibrium and saturation ranges of the wave spectrum, *J. Phys. Oceanogr.*, *31*, 1346–1360, doi:10.1175/1520-0485(2001)031<1346:DDAMSS>2.0.CO;2.

Hwang, P. A., and D. W. Wang (2004), An empirical investigation of source term balance of small scale surface waves, *Geophys. Res. Lett.*, *31*, L15301, doi:10.1029/2004GL020080.

Hwang, P. A., D. W. Wang, E. J. Walsh, W. B. Krabill, and R. N. Swift (2000), Airborne measurements of the directional wavenumber spectra of ocean surface waves. Part 1. Spectral slope and dimensionless spectral coefficient, *J. Phys. Oceanogr.*, *30*, 2753–2767, doi:10.1175/1520-0485(2001)031<2753:AMOTWS>2.0.CO;2.

Jackson, F. C., W. T. Walton, D. E. Hines, B. A. Walter, and C. Y. Peng (1992), Sea surface mean-square slope from K_u-band backscatter data, *J. Geophys. Res.*, *97*, 11,411–11,427, doi:10.1029/92JC00766.

Jones, W. L., L. C. Schroeder, and K. L. Mitchell (1977), Aircraft measurements of the microwave scattering signature of the ocean, *J. Oceanic Eng.*, *2*, 52–61, doi:10.1109/JOE.1977.1145330.

Mouche, A. A., D. Hauser, J. Daloze, and C. Guerin (2005), Dual-polarization measurements at C-band over the ocean: Results from airborne radar observations and comparison with ENVISAT ASAR data, *IEEE Trans. Geosci. Remote Sens.*, *43*, 753–769, doi:10.1109/TGRS.2005.843951.

Munk, W. (2009), An in convenient sea truth: Spread, steepness, and skewness of surface slopes, *Annu. Rev. Mater. Sci.*, in press.

Phillips, O. M. (1984), On the response of short ocean wave components at a fixed wavenumber to ocean current variations, *J. Phys. Oceanogr.*, *14*, 1425–1433, doi:10.1175/1520-0485(1984)014<1425:OTROSO>2.0.CO;2.

Phillips, O. M. (1985), Spectral and statistical properties of the equilibrium range in wind-generated gravity waves, *J. Fluid Mech.*, *156*, 505–531, doi:10.1017/S0022112085002221.

Phillips, O. M., and M. L. Banner (1974), Wave breaking in the presence of wind drift and swell, *J. Fluid Mech.*, *66*, 625–640, doi:10.1017/S0022112074000413.

Vandemark, D., B. Chapron, J. Sun, G. H. Crescenti, and H. C. Graber (2004), Ocean wave slope observations using radar backscatter and laser altimeters, *J. Phys. Oceanogr.*, *34*, 2825–2842, doi:10.1175/JPO2663.1.

Walsh, E. J., D. C. Vandemark, C. A. Friehe, S. P. Burns, D. Khelif, R. N. Swift, and J. F. Scott (1998), Measuring sea surface mean square slope with a 36-GHz scanning radar altimeter, *J. Geophys. Res.*, *103*, 12,587–12,601, doi:10.1029/97JC02443.

Wentz, F. J. (1977), A two scale scattering model with application to the JONSWAP '75 aircraft microwave scatterometer experiment, *Contract Rep. 2919*, 122 pp., NASA, Washington, D. C.

Young, I. R. (1999), *Wind Generated Ocean Waves*, 288 pp., Elsevier, Amsterdam.

P. A. Hwang, Remote Sensing Division, Naval Research Laboratory, 4555 Overlook Avenue, SW, Washington, DC 20375, USA. (paul.hwang@nrl.navy.mil)